PALEOMAGNETISM OF LONAR IMPACT CRATER, INDIA.

Karin L. Louzada[1], Benjamin P. Weiss[2], Adam C. Maloof[3], Sarah T. Stewart[1], Nicholas L. Swanson-Hysell[3] and S. Adam Soule[4]*

[1]Dept of Earth and Planetary Sciences, Harvard University, Cambridge, MA 02138, USA.
[2]Dept of Earth, Atmospheric and Planetary Sciences, Massachusetts Institute of Technology, Cambridge, MA 02139 USA.
[3]Dept of Geosciences, Princeton University, Princeton, NJ 08544, USA.
[4]Woods Hole Oceanographic Institution, Woods Hole, MA 02540, USA.
*Corresponding author: K. L. Louzada (louzada@fas.harvard.edu).
Department of Earth and Planetary Sciences, Harvard University, 20 Oxford Street, Cambridge, MA 02138, USA, tel. 617-495-8986, fax. 617-495-0635.

SUPPLEMENTAL ONLINE MATERIAL

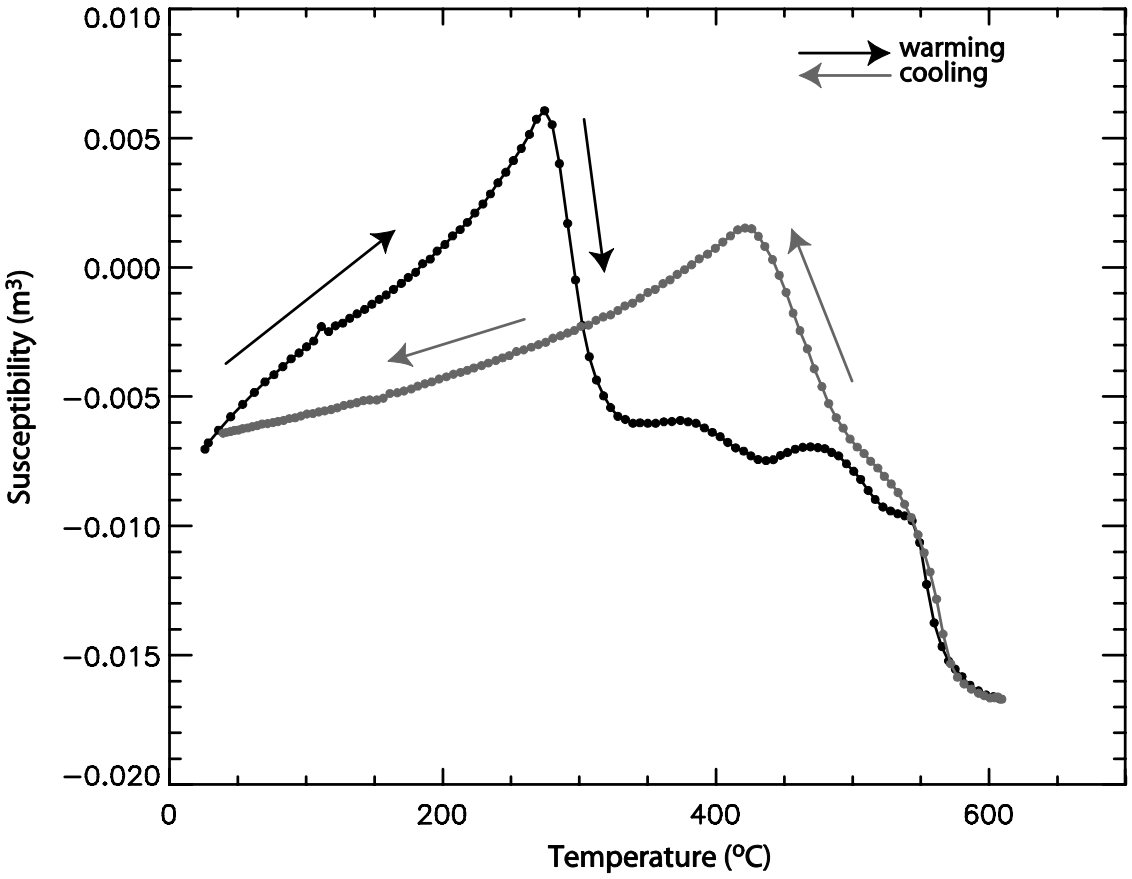

Figure 1S: Susceptibility as a function of temperature (in an argon atmosphere) for the background Deccan flow at Pimpalner Dam (2205793 N, 664208 E, 8.1 Rc). The curve shows 1) an irreversible increase in susceptibility at ~275°C indicative of oxidized titanomagnetite and 2) a reversible decrease in susceptibility at 580°C (Curie temperature) indicative of magnetite. The measurements were performed on an Agico MFK1-FA susceptibility-meter with CS-3 heater at CEREGE, CNRS, France.

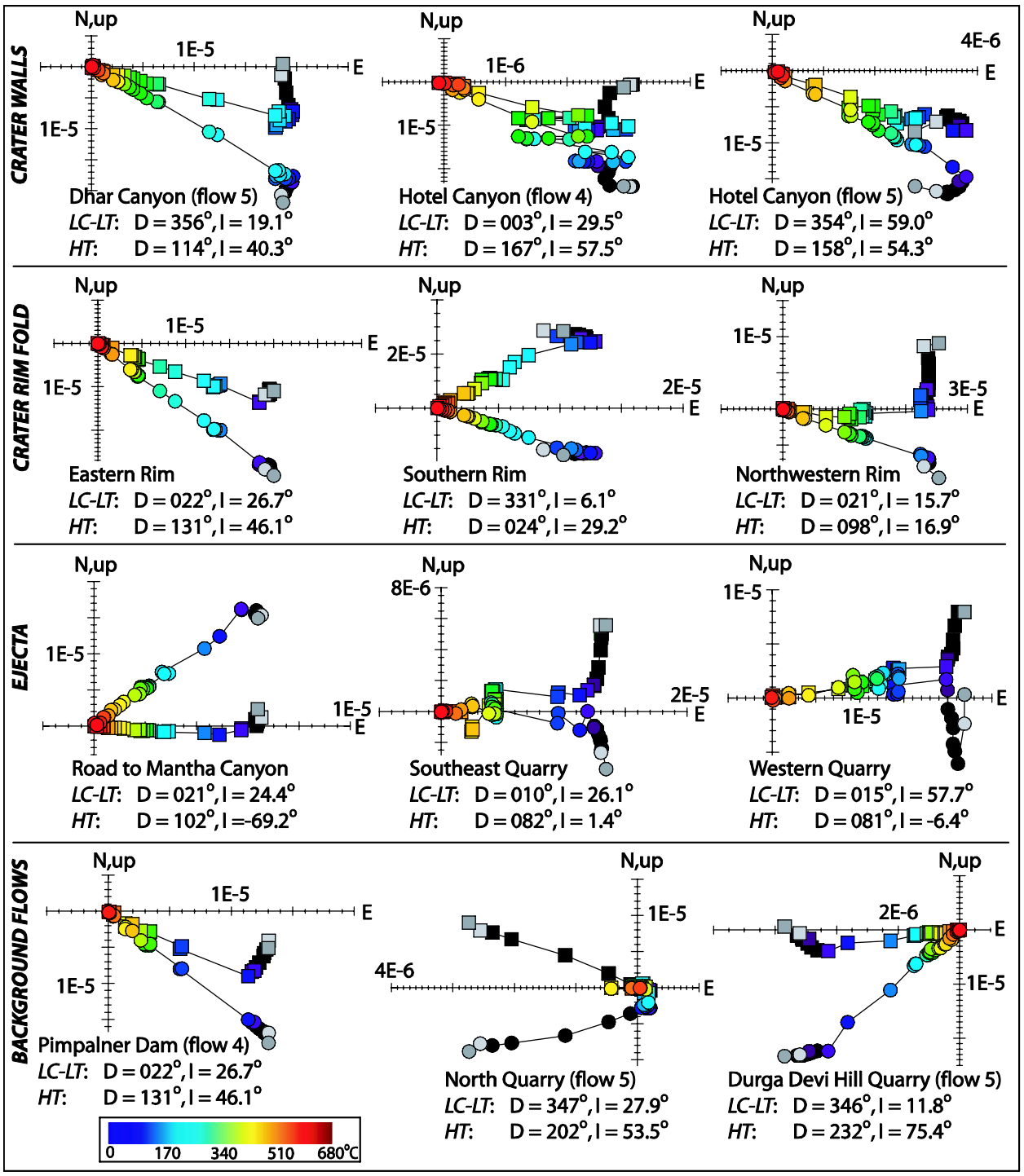

Figure 2S: Orthogonal (Zijderveld, 1967) projections of some representative samples. The data are plotted in geographic coordinates. The results are from 'AF+TH' experiments: dark grey - NRM, light grey - low temperature treatment, black - alternating field treatment, and color - step-wise heating. Squares are 'N and E' projections, circles are 'up and E' projections. Note the differences in scales of the plots. Units are Am^2. See Figure 1 and Table 1S for the geographic locations of the sampling sites.

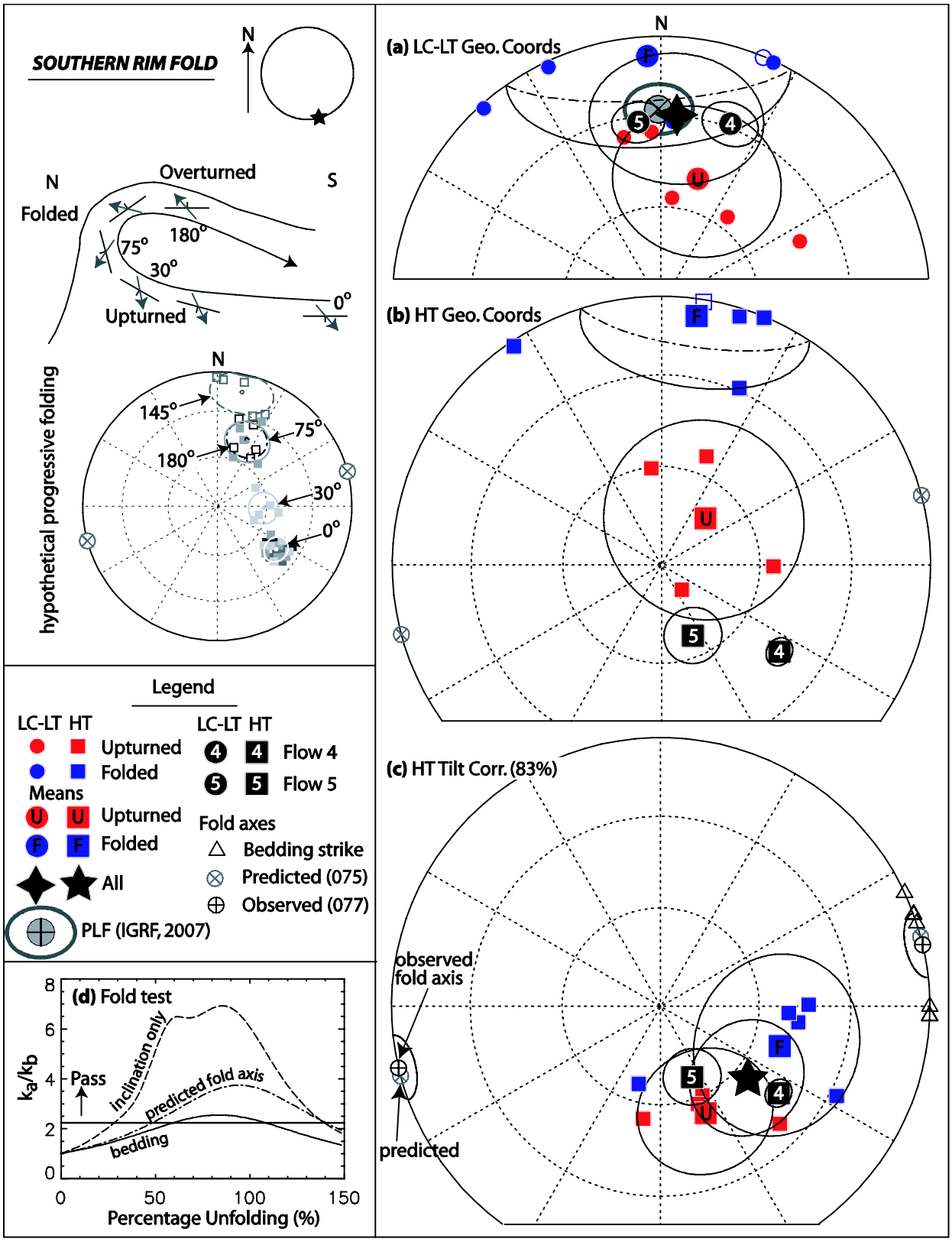

Figure 3S: See figure caption on page 7.

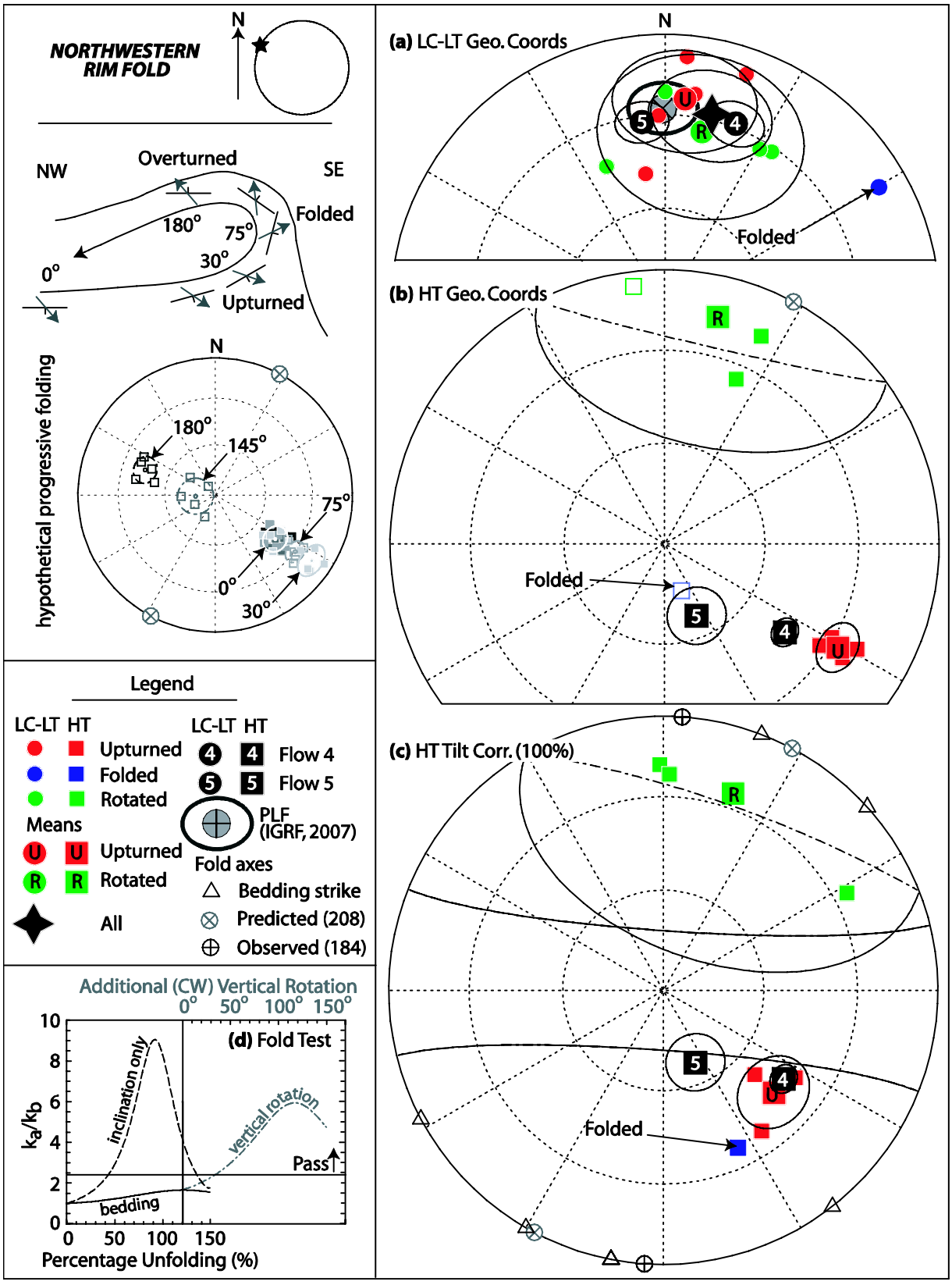

Figure 4S: See figure caption on page 7.

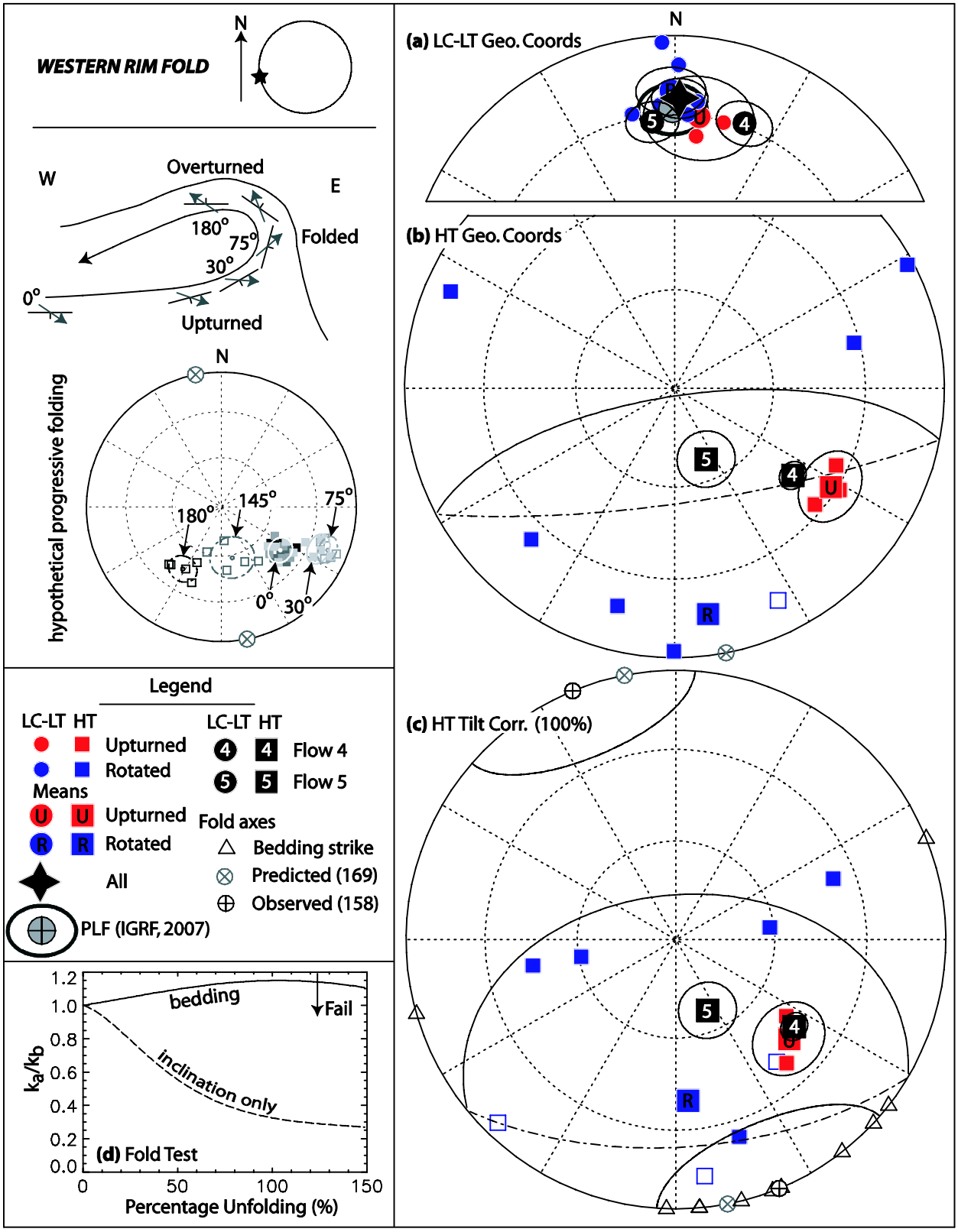

Figure 5S: See figure caption on page 7.

Figures 3S-5S: Fold analyses of the Southern Rim (Figure 3S), Northwestern Rim (Figure 4S) and Western Rim (Figure 5S). The top left cartoons indicate the locations of the fold sites and the hypothetical progressive change in direction of the *HT* component in flow 4 as a result of folding about the azimuths of the crater rim, in cross section and in equal area projection. Note the switch from lower to upper hemisphere with increasing folding. (a) Equal-area projection of *LC*-*LT* (circles) in geographic coordinates. (b) *HT* directions (squares) in geographic coordinates. (c) *HT* directions after tilt correction (squares) about the bedding strike (open triangles). Open symbols and dash-dotted confidence ellipses denote upper hemisphere. Samples are subdivided into groups depending on their bedding dip and *HT* directions:

- in Figure 3S: upturned = dip 30°-75°, folded = dip 75°-180°
- in Figure 4S: upturned = dip 30°-75°, folded = dip 75°-180° (one sample), vertically rotated = *HT* directions in geographic coordinates are approximately 90 degrees from their expected directions.
- in Figure 5S: upturned = dip 30°-75°, vertically rotated = *HT* directions in geographic coordinates do not correspond with their expected direction.

(d) Results of fold-test analyses (precision parameter k_a relative to the initial k_b): solid line = unfolding about the individual sample bedding by the dip; dash-dot line = folding about the predicted fold axis by the dip; dashed line = inclination only results of folding about the bedding by the dip.

N.B.: In Figure 5S, the rotated rim blocks pass the conglomerate test: the length of the resultant vector after tilt correction (3.91) remains below the maximum length allowed for randomness (4.48 with 95% confidence, for 8 samples).

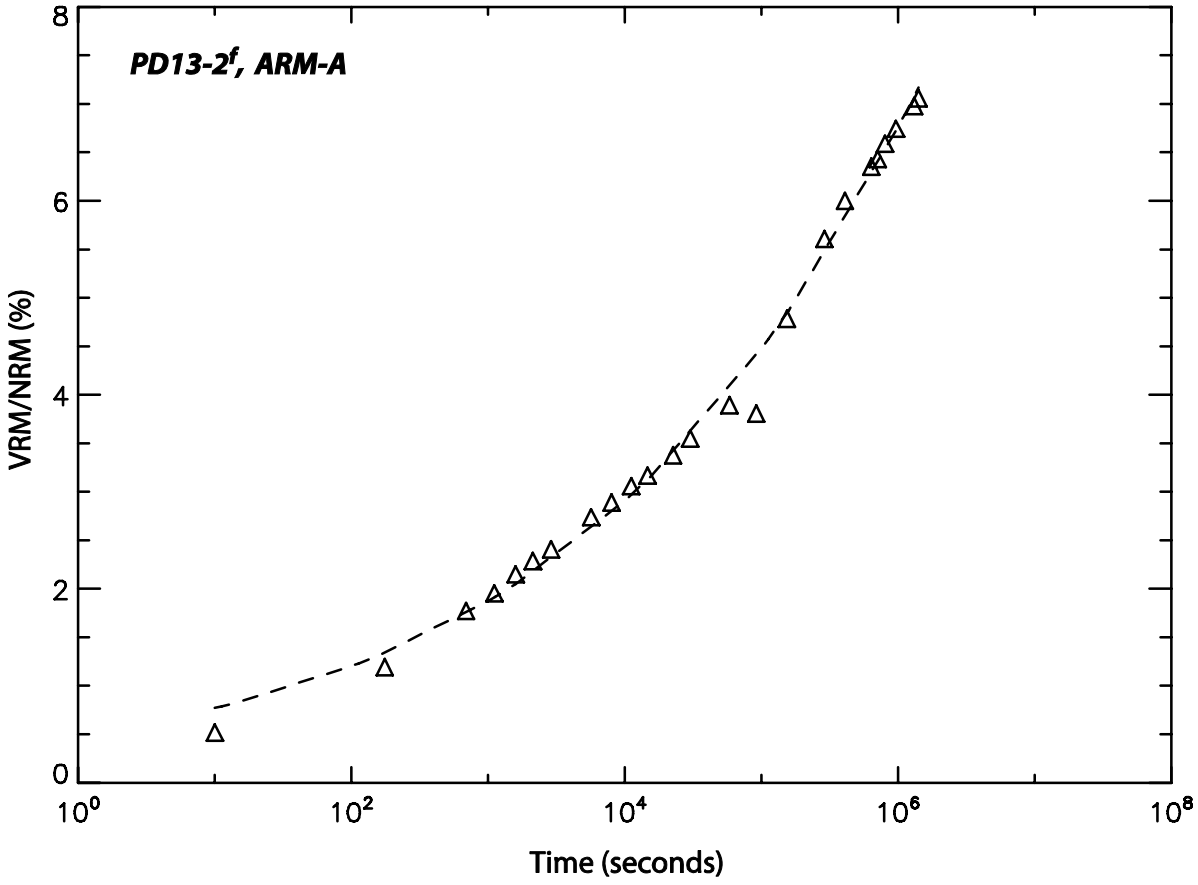

Figure 6S: An example result of VRM acquisition experiments ('VRMacq') for a background basalt from flow 4 at Pimpalner Dam (2205793N, 664208E). The initial state of the specimen prior to VRM acquisition in a 47 μT field was anhysteric remanent magnetization (ARM) acquired in an alternating field of 200 mT and a 0.5 mT bias field. The acquisition of VRM is non-linear with log(time) and was fit to a hyperbolic tangent of the following form: $VRM = A * \tanh(B * t^n)$ (afterBowles and Johnson, 1999), where *VRM* is in A/m, *B* and *n* are dimensionless, and *t* is in seconds.

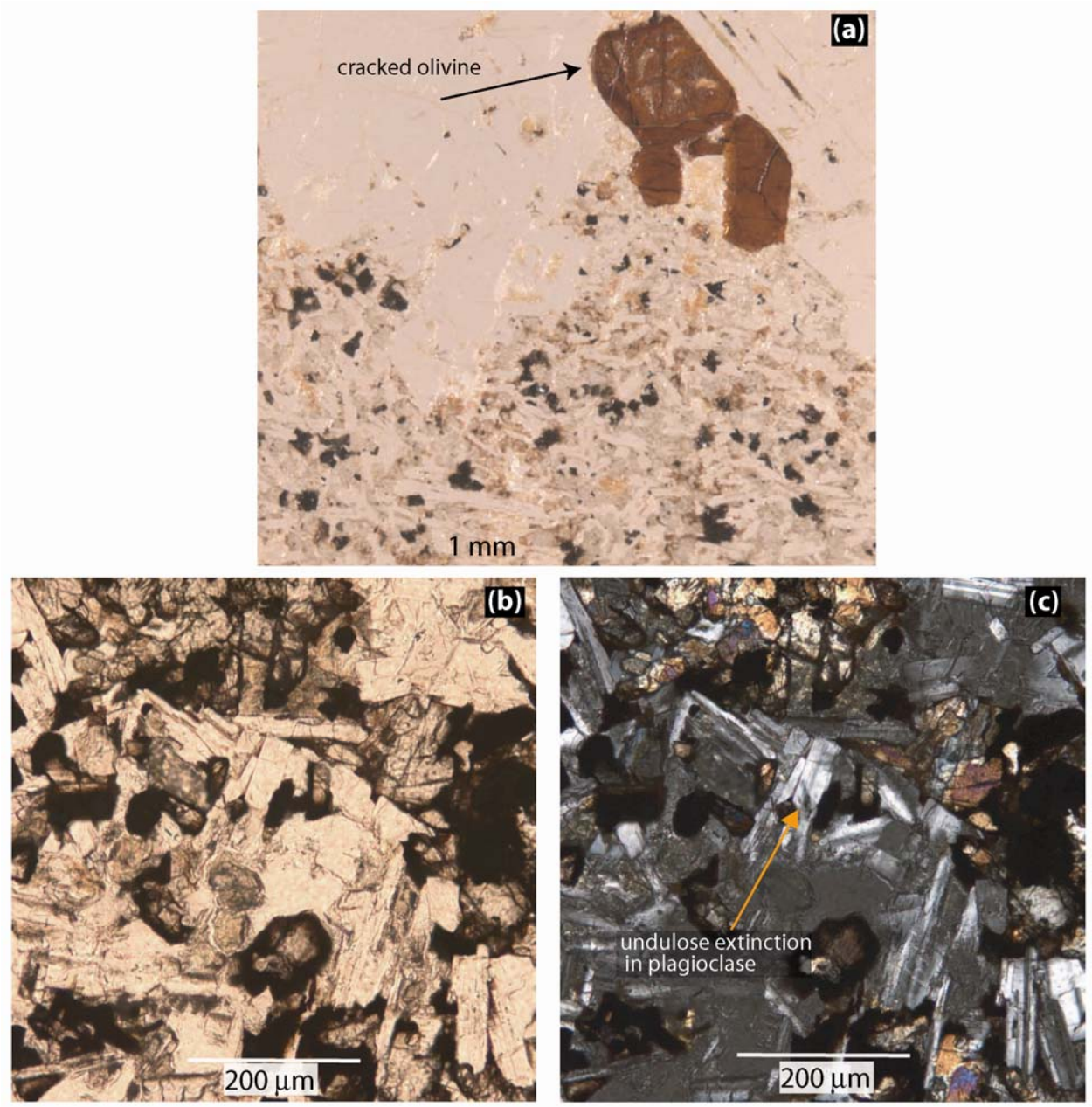

Figure 7S: Photomicrographs of two thin-sections from ejecta blocks from the Telcom Pit site (2211086N, 657941E). (a) Reflected light image showing cracked, altered olivine phenocrysts (arrow). Transmitted light image in (b) plane-polarized light and (c) cross-polarized light showing slight undulose extinction in plagioclase phenocrysts (arrow).

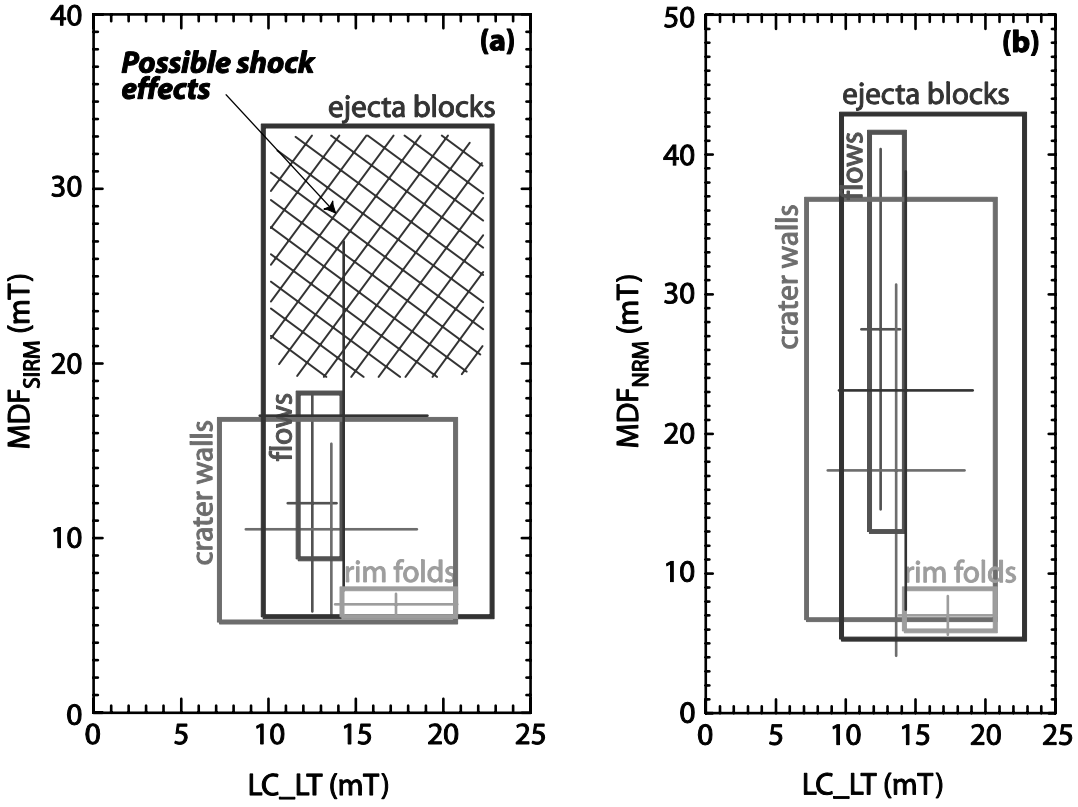

Figure 8S: Peak unblocking coercivity of LC_LT versus (a) MDF of SIRM and (b) MDF of NRM from the 'Rockmag' experiments. Crosses indicate the averages (± 1σ) of measurements and the bounding boxes the minimum and maximum measured values. The hatched region indicates where shock effects may be realized.

Table 1S: Geographic locations of the paleomagnetic sites. (UTM, WGS 84)

Site name	*Site type*	*N (m)*	*E (m)*	*d (Rc)*
Hotel Canyon	Crater wall	2209475	658688	0.91
Dhar Canyon	Crater wall	2210479	658325	1.07
Eastern Rim	Rim fold	2209274	658709	0.99
Southern Rim	Rim fold	2208724	658112	1.00
Western Rim	Rim fold	2209432	656901	1.08
Northwestern Rim	Rim fold	2210048	657047	1.02
Road to Mantha Canyon	Ejecta	2208087	658301	1.73
Kalapani Dam	Ejecta	2208333	656244	2.26
Little Lonar	Ejecta	2211333	658071	1.89
Southeast Quarry	Ejecta	2208545	658693	1.47
Telcom Pit	Ejecta	2211086	657941	1.61
Western Quarry	Ejecta	2209746	656118	1.92
Kalapani Dam	Background flow 4	2208231	656085	2.47
North Quarry	Background flow 5	2212187	659304	3.22
Durga Devi Hill Quarry	Background flow 5	2209050	660642	3.09
Pimpalner Dam	Background flow 4	2205793	664208	8.09

d=Distance from crater center in crater radii (1 Rc = 0.94 km).

Table 2S: Paleomagnetic Directions

	D°	*I*°	*k*	α_{95}°	*R*	*Reference*
Primary Component (*HT*)						
Background Flow 2 (3)	164.4	+49.5	84.1	13.5	2.9	
Background Flow 3 (1)	169.3	+52.7	--	--	--	
Background Flow 4 (32)	126.4	+44.7	38.6	4.1	31.1	
Background Flow 5 (29)	156.0	+66.5	10.5	8.6	26.3	
Mean Background Flows (65)	**137.9**	**+55.4**	**12.1**	**5.2**	**59.7**	**This study**
Lonar Lake – Crater Walls	136	+42	71.4	5.2	--	Poornachandra Rao and Bhalla, 1984
Lonar Lake – Crater Rim (Flow 4 - uncertain)*	128	+38	56.2	9.5	--	Pal and Ramana, 1972
PaleoDeccan Direction at Lonar	157.6	+47.4	--	1.9	--	After Vandamme, et al., 1991a
Aurangabad – Deccan Basalt Flows (19°51'N,75°16'E)	150	+48	26	5.5	--	Athavale and Anjaneyulu, 1972
Jalna (19°50'N, 75°56'E) – Deccan Basalt Flows	160	+46	32	3.8	--	Pal and Bhimasankaram, 1971
Secondary Component (*LC-LT*)						
Background Flow 2 (3)	6.4	+28.2	207.1	8.5	2.9	
Background Flow 3 (1)	12.9	+21.8	--	--	--	
Background Flow 4 (32)	20.9	+28.6	12.3	7.5	29.4	
Background Flow 5 (30)	352.6	+32.0	14.9	7.0	28.0	
Mean Background Flows (66)	**7.4**	**+30.7**	**11.2**	**5.5**	**60.2**	**This study**
Lonar Lake – Crater Walls	9	+47	47.6	6.4	--	Poornachandra Rao and Bhalla, 1984
PLF	-0.8	+28.0	--	8.8**	--	IGRF, 2007; Elmaleh, et al., 2004

D = declination, *I* = inclination, *k* = precision parameter, α_{95} = radius of 95% confidence, and *R* = length of the resultant vector. The number of samples in each group is indicated in parentheses. *Averaged over geographic coordinates from 6 sites along the crater rim with azimuths ranging from 320° to 140°. *Based on secular variation for the past 10 kyrs.

Table 3S: Viscous Remanent Magnetization Acquisition Results

Sample	*Type*	*α (°)*	*NRM (A/m)*	*A (A/m)*	*B*	*n*	*NRM/VRM @ 50kyr*
LSEQ-5-2[e]	NRM[A]	11	8.29	3.14E-01	1.33E-02	0.306	0.038
PD-3-1[f]	NRM[A]	21	5.17	4.45E-01	8.42E-03	0.237	0.088
PD-3-1[f]	NRM[D]	21	5.17	7.53E-02	8.50E-03	0.362	0.015
LHC5-5-4[w]	NRM[A]	59	2.91	3.79E-01	4.65E-03	0.411	0.13
LHC5-5-4[w]	NRM[D]	59	2.91	2.35E-01	2.32E-02	0.331	0.081
PD-13-2[f]	ARM[A]	105	3.75*	6.28E-01	2.95E-02	0.194	0.17
PD-13-2[f]	AF85[A]	105	6.24	3.40E-02	3.52E-02	0.268	0.0054
PD-13-2[f, **]	AF85[A]	105	6.49	2.65E-02	7.99E-02	0.253	0.0048
LWO1-1-2[r]	NRM[A]	113	3.36	1.01E-01	4.44E-03	0.441	0.030
LTP1-11-2[e]	AF85[A]	118	1.60	1.43E+00	9.03E-03	0.326	0.89

[e] ejecta clasts, [f] background flow, [r] rim fold, [w] crater wall, [A] acquisition, [D] decay.
*ARM:200 mT AF + 0.05 mT bias field
**Short data set (0.1 day).
NRM = natural remanent magnetization, untreated.
ARM = anhysteric remanent magnetization, AF 200 mT and bias field 0.5 mT.
AF85 = alternating field demagnetized with a peak AF field of 85 mT.

Table 4S: Rock Magnetic Parameters

	NRM (A/m)	*SIRM (A/m)*	*MDF of NRM (mT)*	*MDF of SIRM (mT)*	*Reference*
Lonar Basalts					
Background Flows* (4)	**4.07 (2.38-5.28)**	**834 (681-986)**	**27.5 (13.0-41.6)**	**12.0 (8.8-18.3)**	
Crater Walls* (5)	**5.00 (2.69-8.61)**	**862 (552-1170)**	**17.4 (6.7-36.8)[4]**	**10.5 (5.2-16.8)**	
Crater Rim Folds* (4)	**18.5 (5.43-44.2)[3]**	**670 (567-765)[3]**	**7.0 (5.9-8.9)**	**6.2 (5.5-7.1)**	
Ejecta Clasts* (7)	**8.67 (2.12-21.8)**	**922 (577-1190)**	**23.1 (5.3-42.9)[5]**	**17.0 (5.5-33.6)**	**This study**
Impact Spherules*	0.856, 0.0307	>580, 4.52	--	--	Weiss, et al., 2007
Basalt in, on and outside the crater rim*	4.8 (1.5-12.8)	1041 (580-1624)	--	16.9 (7.2-26.3)	Cisowski and Fuller, 1978
Upper Crater Walls	4.7 (4.0-5.6)	286 (237-348)	20.2 (4.1-31.2)	13.6 (7.1-17.3)	Poornachandra Rao and Bhalla, 1984
Lower Crater Walls	3.4 (2.5-4.7)	177 (163-191)	9.2 (3.8-26.7)	7.8 (4.9-11.7)	Poornachandra Rao and Bhalla, 1984
Crater Rim	--	--	34.6 (31.8-38.1)	--	Pal and Ramana, 1972
Other Deccan Localities					
Aurangabad (19°51'N, 75°16'E)	9.38 (2.14-30.59)	--	12.3 (1.9-25.4)	--	Athavale and Anjaneyulu, 1972
Jalna (19°50'N, 75°56'E)*	2.5-9.9	--	--	--	Pal and Bhimasankaram, 1971
Nagpur-Bombay	3.4 (0.1-10)	--	~20	--	Vandamme, et al., 1991b

Rock magnetic parameters, mean and range in parenthesis. *NRM* = natural remanent magnetization, *SIRM* = saturation isothermal remanent magnetization, and *MDF* = median destructive field. Parentheses indicate number of specimens in the set unless the number is otherwise stated as [3],[4] or [5].
*Converted to SI units assuming a density of 2.9 g/cm^3 (Fudali, et al., 1980).

References

Athavale, R.N., Anjaneyulu, G.R., 1972. Palaeomagnetic results on Deccan Trap lavas of the Aurangabad region and their tectonic significance. Tectonophysics 14, 87-103.

Bowles, J., Johnson, H.P., 1999. Behavior of oceanic crustal magentization at high temperatures: Viscous magnetization and the marine magnetic anomaly source layer. GRL 26, 2279-2282.

Cisowski, S.M., Fuller, M., 1978. The Effect of Shock on the Magnetism of Terrestrial Rocks. JGR 83, 3441-3458.

Elmaleh, A., Valet, J.-P., Quidelleur, X., Solihin, A., Bouquerel, H., Tesson, T., Mulyadi, E., Khokhlov, A., Wirakusumah, A.D., 2004. Palaeosecular variation in Java and Bawean Islands (Indonesia) during the Bruhnes chron. GJI 157, 441-454.

Fudali, R.F., Milton, D.J., Fredriksson, K., Dube, A., 1980. Morphology of Lonar Crater, India: Comparisons and Implications. The Moon and the Planets 23, 493-515.

IGRF, International Geomagnetic Reference Field, 2007.

Pal, P.C., Bhimasankaram, V.L.S., 1971. Palaeomagnetism of the Deccan Trap flows of Jalna, India. EPSL 11, 109-112.

Pal, P.C., Ramana, C.V., 1972. Lonar Lake - Volcanic Crater or Astrobleme. C.E.G. Bulletin 114-121.

Poornachandra Rao, G.V.S., Bhalla, M.S., 1984. Lonar Lake: palaeomagnetic evidence of shock origin. Geophysical Journal Royal astronomical Society 77, 847-862.

Vandamme, D., Courtillot, V., Besse, J., Montigny, R., 1991a. Paleomagnetism and age determinations of the Deccan Traps (India): Results of a Nagpur-Bombay traverse and review of earlier work. Reviews of Geophysics 29, 159-190.

Vandamme, D., Courtillot, V., Besse, J., Montigny, R., 1991b. Paleomagnetism and Age Determinations of the Deccan Traps (India): Results of a Nagpur-Bombay Traverse and Review of Earlier Work. Reviews of Geophysics 29, 159-190.

Weiss, B.P., Garrick-Bethell, I., Pederson, S., Louzada, K.L., Stewart, S.T., Maloof, A.C., Paleomagnetism of Impact Glass from Lonar Crater, India, Lunar and Planetary Science Conference XXXVIII, League City, TX, 2007, p. Abstract #: 2360.